

Optical Properties of a Semimagnetic Quantum Well in a Proximity of a Superconducting Film

K.M. LEBECKI*, Ł. KŁOPOTOWSKI AND J. KOSSUT

Institute of Physics, Polish Academy of Sciences
al. Lotników 32/46, 02-668 Warsaw, Poland

We consider, via numerical calculations, a hybrid structure made of a semimagnetic $\text{Cd}_{1-x}\text{Mn}_x\text{Te}$ quantum well deposited in a close proximity to superconducting niobium film. We simulate photoluminescence and the Faraday rotation spectra, modified by the presence of vortices in this type II superconductor. The magnitude of the evaluated effects is small — the vortex induced spectral line shape variation is of the order of 1% at 1 K and 0.1% at 3 K and is expected to occur mainly in the field range between 0.03 T and 0.05 T.

PACS numbers: 78.67.De, 74.25.Qt

1. Introduction

Diluted magnetic semiconductors (DMSs) are known for their large Zeeman splitting [1]. The idea of placing magnetic structures (like ferromagnetic islands or type I superconductors) in the proximity of a DMS layer and using this layer as a magneto-optical detector of a magnetic field can be found in many papers [2–5]. In this paper, we consider the influence of a type II superconductor (SC) on optical properties of a DMS quantum well (QW). When an external magnetic field is applied perpendicularly to the SC layer, it penetrates the layer in the form of vortices each carrying the magnetic flux quantum. Increasing the external magnetic field results in an increase in the vortex density. Therefore, the magnetic field distribution in the QW is spatially modulated and depends on the external magnetic field. By numerical calculations, we simulate the optical response, namely the excitonic photoluminescence (PL) and Faraday rotation (FR) spectra, of such QW.

*corresponding author; e-mail: lebecki@ifpan.edu.pl

2. Calculation details

We consider a hybrid structure consisting of Nb layer deposited on top of a DMS QW made of $\text{Cd}_{1-x}\text{Mn}_x\text{Te}$ (Fig. 1b). We chose Nb due to its high magnetic field in the vortex core [6]. Parameters characterizing optical properties of the QW are: manganese concentration — $x(\text{Mn})$, PL line width (FWHM) — w , QW thickness — d , dielectric constant — ε_∞ , exciton energy — E_0 , resonance amplitude — A , and the resonance width — Γ . Parameters characterizing the SC layer are the coherence length — ξ and the penetration depth — λ . The calculations are performed for three samples with parameter values presented in the Table. For the material parameters see Refs. [7–11].

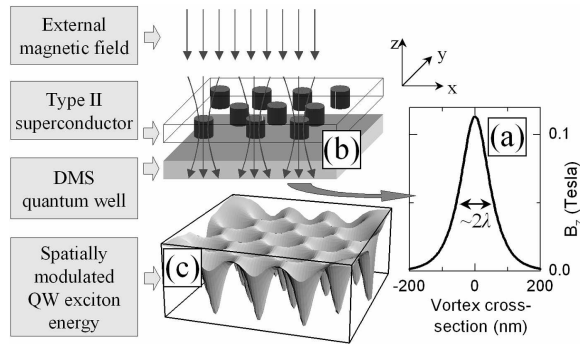


Fig. 1. (a) Cross-section through a single superconducting vortex. Magnetic field (vertical axis) is concentrated in the vortex center. (b) Schematic diagram of evaluated samples. Superconducting film, containing vortices, is placed close to a QW. (c) Lower excitonic level of the QW, spatially modulated due to vortex field penetrating the QW. Potential minima exceed -4 meV in this case. Calculation results for the sample A, $T = 0.1$ K, $B = 0.04$ T.

We determine the spatial distribution of the magnetic field inside the QW in a following way. The field inside a single vortex is calculated using the Clem's model [12] (Fig. 1a). The vortices are assumed to form a regular and static hexagonal Abrikosov lattice [13], where the inter-vortex distance is determined only by the external magnetic field. We neglect the SC–QW distance and take the field inside the QW as equal to that inside the SC, i.e., we disregard the field spreading shown schematically by bent arrows in Fig. 1b. In a realistic experiment, the SC–QW spacer would be approximately 10 nm wide. The peak width of the field profile inside the vortex, 2λ ([12], see Fig. 1a), is of the order of 100 nm, and therefore our assumption is well justified.

We model an experiment, where the observation spot is larger than the inter-vortex distance and therefore we average the optical response over the sample surface. The PL intensity emitted by the QW, $PL_{\text{QW}}(E, E_0)$, is assumed to have a Gaussian spectrum, where E is the photon energy and E_0 — the peak center

TABLE

Samples used in the calculations. See the text for the explanation of the parameters.

Sample	SC properties	$x(\text{Mn})$	w (meV)	Faraday effect parameters
A	$\xi(0) = 41$ nm, $\lambda(0) = 39$ nm	0.64%	3.25	$d = 8$ nm, $\varepsilon_\infty = 7.29$, $E_0 = 1652.2$ meV, $A = 7.75$ meV, $\Gamma = 3.6$ meV
B	$\xi(0) = 41$ nm, $\lambda(0) = 75$ nm	0.64%	3.25	$d = 8$ nm, $\varepsilon_\infty = 7.29$, $E_0 = 1652.2$ meV, $A = 7.75$ meV, $\Gamma = 3.6$ meV
X	$\xi(0) = 41$ nm, $\lambda(0) = 39$ nm	1%	1.5	—

(exciton level). We consider only one excitonic state — the lowest QW level, heavy hole exciton in the $1s$ state in the lower spin subband. We model the peak position dependence on the magnetic field, $\Delta E(B)$, by the modified Brillouin function [14]. We assume that the magnetic field shifts only the peak position and does not modify its intensity. The calculations of the PL spectrum for the SC–QW hybrid, $PL_{\text{SC-QW}}$, are done by integrating a convolution of functions $PL_{\text{QW}}(E, E_0)$ and $\Delta E(B)$ over the sample surface:

$$PL_{\text{SC-QW}}(E, E_0) = \int \int PL_{\text{QW}}(E, E_0 - \Delta E(B(x, y))) dx dy,$$

where $B(x, y)$ is the field distribution inside the QW.

To calculate the excitonic FR, we consider a two-level system described by complex dielectric functions $\varepsilon^\pm(E, E_0)$ corresponding to two circular light polarization, σ^+ and σ^- . $\varepsilon^\pm(E, E_0)$ have Lorentzian energy dependences [15, 7] and we assume that the magnetic field affects only the resonance energy position and does not change its width and amplitude. From complex $\varepsilon^\pm(E, E_0)$ we obtain the refraction and extinction coefficients and the FR is proportional to the difference of refraction indices for σ^+ and σ^- polarizations:

$$\Theta_{\text{QW}}(E, E_0) = \frac{Ed}{2\hbar c} [n(E, E_0 - \Delta E(B)) - n(E, E_0 + \Delta E(B))].$$

To calculate the FR for the SC–QW hybrid, we first compute separately two components of the electrical field vector of the transmitted light, ε_x , ε_y . This is done in a similar way, as in the above-mentioned case of the PL calculations:

$$\varepsilon_x(E) = \int \int \sin \left(\frac{Ed}{2\hbar c} (n(E, E_0 - \Delta E(B(x, y))) - n(E, E_0 + \Delta E(B(x, y)))) \right) dx dy,$$

$$\varepsilon_y(E) = \int \int \cos \left(\frac{Ed}{2\hbar c} (n(E, E_0 - \Delta E(B(x, y))) - n(E, E_0 + \Delta E(B(x, y)))) \right) dx dy.$$

Finally, the FR spectrum for the hybrid is given by

$$\Theta_{\text{SC-QW}}(E) = \arctan(\varepsilon_x(E)/\varepsilon_y(E)).$$

3. Results and discussion

A simulation of the PL spectrum for the QW–SC hybrid (sample X) calculated for $B = 0.04$ T is shown in the inset B of Fig. 2 (open symbols). For comparison, a QW-only spectrum is also shown (solid line). The presence of the SC layer results in: (i) reduction of the Zeeman shift, (ii) lowering the intensity and broadening of the peak, and (iii) introducing a non-symmetrical peak shape. The reduction of the Zeeman shift is caused by a partial field screening, as the field is concentrated around the vortex cores. It can be seen in Fig. 2, where the PL peak centers of QW-only and the QW–SC hybrid (sample A) are plotted versus magnetic field. The influence of vortices is the strongest in the marked region of magnetic fields between 0.03 T and 0.05 T. To quantify the influence of vortices on the PL line shape, we plotted (inset B in Fig. 2) the variation of the PL line width defined as $\Delta w/w = |w_{\text{QW}} - w_{\text{QW-SC}}|/w_{\text{QW}}$. In the marked region $\Delta w/w$ reaches almost 20%. This increase is due to the magnetic field inhomogeneity caused by

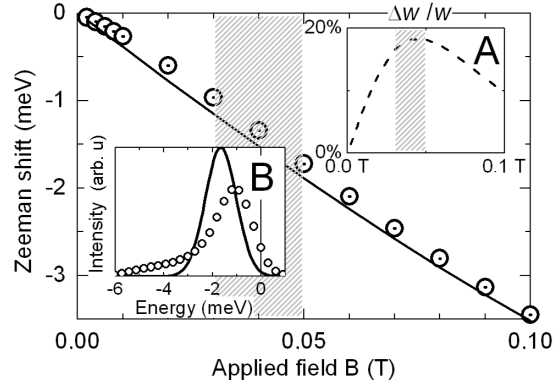


Fig. 2. Calculated PL Zeeman shift at $T = 0.1$ K of the lower QW exciton level versus magnetic field. Hybrid structure (sample A) QW–SC — open symbols, QW-only — solid line. The vortices decrease slightly the Zeeman shift, especially in the marked field region. Inset A: the PL line width modification $\Delta w/w$ as a function of the magnetic field. Inset B: the PL spectrum for $B = 0.04$ T and the sample X. The vertical axis: intensity, the horizontal axis: relative energy — zero corresponds to the peak position at zero field.

the presence of vortices. The deviation of the spectrum from the Gaussian shape is directly related to the presence of the vortex field, which reaches 0.1 T in the vortex core. The low energy shoulder of the PL peak is due to the recombination of the excitons located in the potential minima created by the vortex field (cf., Fig. 1c).

In Fig. 3 we show the maximum Faraday angle, $\theta(E_0)$, versus the external magnetic field, calculated for sample A. The decrease of the FR in the QW-SC hybrid, with respect to QW-only, is a result of the Zeeman splitting reduction discussed above. The difference $|\theta_{\text{QW}} - \theta_{\text{QW-SC}}|$ is the largest in the same region of magnetic fields — between 0.03 T and 0.05 T. Beside a FR peak decrease, a small broadening of the FR spectrum, $\theta_{\text{QW-SC}}(E)$, can be observed (not shown here). This broadening results from the inhomogeneous field penetrating the QW. In the inset of Fig. 3 we show $\Delta\theta/\theta = |\theta_{\text{QW}} - \theta_{\text{QW-SC}}|/\theta_{\text{QW}}$ as a function of the magnetic field. In the region of interest — between 0.03 and 0.05 T — the values of $\Delta\theta/\theta$ amounts roughly to 15%, which is comparable to the PL line width increase computed for the same conditions. We will use this quantity to compare the sensitivity of PL and FR methods (see below).

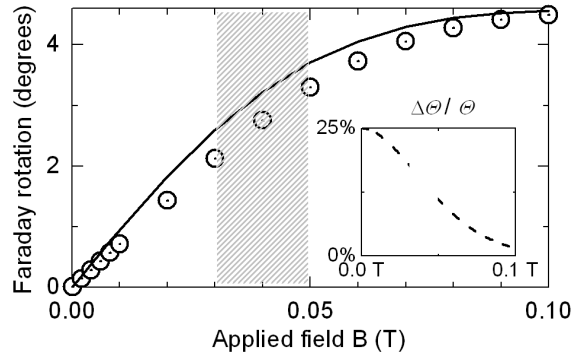


Fig. 3. The FR versus the magnetic field for the sample A in two cases: QW-SC — open symbols, QW-only — solid line. The vortices decrease the rotation angle, especially in the marked field region. The inset shows $\Delta\theta/\theta$. $T = 0.1$ K.

Both PL and FR data show the largest vortex-induced modifications in the range between 0.03 and 0.05 T. For larger fields these modifications are smaller because the vortices start to overlap leading to flattening of the spatial field modulation in the QW (see Fig. 7 in Ref. [16]). Consequently, the vortex-induced modifications of the PL and FR spectra are weaker. Indeed, the inter-vortex distance $\sqrt{2/\sqrt{3}}\sqrt{\Phi_0/B}$ [6] (where Φ_0 is magnetic flux quantum) is equal to the vortex field diameter 2λ at the magnetic field of about 0.1 T for $\lambda = 40$ nm (see the Table).

To compare the sensitivity of PL and FR methods in a quantitative way, we plot $\Delta\theta/\theta$ and $\Delta w/w$, both computed for $B = 0.04$ T, versus temperature

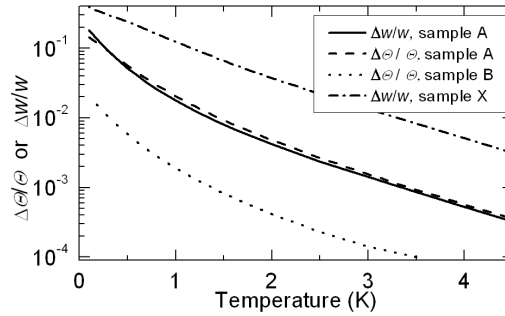


Fig. 4. Vortex influence on the optical properties as a function of the temperature — simulations for various samples. Vertical axis shows the ratio $\Delta\theta/\theta$ or $\Delta w/w$. Solid and dashed lines: sample A, the dotted line: sample B, the dash-dotted: sample X. Solid and dash-dotted lines represent $\Delta w/w$, while dashed and dotted lines: $\Delta\theta/\theta$ $B = 0.04$ T.

for three considered samples, see Fig. 4. The solid and the dashed line show the results of FR and PL calculations done for sample A. First of all, strong temperature dependence can be seen, a change of sensitivity of two orders of magnitude between 1 and 4 K is obtained. Secondly, the influence of vortices on both PL and FR is, surprisingly, comparable. The dotted line shows Faraday rotation for sample B which is characterized by a larger penetration depth — the vortex field peak is lower and broader. It is seen that the increase in λ by a factor of roughly two decreases the sensitivity by an order of magnitude. On the other hand, the dash-dotted curve shows the PL line width calculated for the sample X, which has a higher Mn concentration and a narrower line width — with respect to samples A and B. In this case, the sensitivity is increased by an order of magnitude. Concluding, for samples with relatively narrow PL lines and relatively high Mn content, the vortex induced modifications in PL and FR can reach 1% for $T = 1$ K and 0.1% for $T = 3$ K.

Although the FR is usually a more sensitive technique than the PL, the results presented here might be explained by the fact that for the FR the integration over the modulated region means averaging the rotation angle (as long as we neglect any ellipticity / depolarization effects). We point out that the experimental detection of the effects evaluated here is difficult, as vortex-induced reduction of the Zeeman splitting can be confused with the effect of magnetic ion heating [17]. Moreover, the PL spectrum contains more than one peak. For instance, the charged exciton transition, usually appears a few meV below the neutral exciton transition and therefore can easily dominate and obscure the expected phenomena (inset B in Fig. 2). The assumption of small SC-DMS distance leads to overestimation of the expected effects. For larger distances, the vortex-induced fluctuations are smaller and the field distribution in QW is more flattened.

4. Conclusions

We calculated photoluminescence and Faraday rotation for a hybrid consisting of a $\text{Cd}_{1-x}\text{Mn}_x\text{Te}$ quantum well placed in the proximity to a type II superconducting layer. The vortices, present in the superconductor, influence the optical properties mainly in a low magnetic field range (0.03 ÷ 0.05 T). These small effects strongly depend on the temperature. Their observation requires a quantum well with a concentration of Mn enabling a large Zeeman splitting and still possessing a narrow photoluminescence and absorption line widths. Simultaneously, in order to have a large magnetic field modulation in the quantum well, it is necessary to have a type II superconductor characterized with a possibly small penetration depth.

Acknowledgments

We acknowledge the support from the Foundation for Polish Science through a Subsidy 8/2003. We thank G. Karczewski for critical reading of the manuscript.

References

- [1] J. Kossut, W. Dobrowolski, in: *Handbook of Magnetic Materials*, Vol. 7, Ed. K.H.J. Buschow, Elsevier Science Publishers B.V., Amsterdam 1993, ch. 4, p. 286.
- [2] J. Kossut, I. Yamakawa, A. Nakamura, G. Cywiński, K. Fronc, M. Czczcott, J. Wróbel, F. Kyrychenko, T. Wojtowicz, S. Takeyama, *Appl. Phys. Lett.* **79**, 1789 (2001).
- [3] A. Kudelski, K. Fronc, J. Wróbel, S. Maćkowski, G. Cywiński, M. Aleszkiewicz, F. Kyrychenko, T. Wojtowicz, J. Kossut, J. Gaj, *Solid State Commun.* **120**, 35 (2001).
- [4] C. Gourdon, V. Jeudy, M. Menant, D. Roditchev, A.T. Le, E.L. Ivchenko, G. Karczewski, *Appl. Phys. Lett.* **82**, 230 (2003).
- [5] F. Pulizzi, P.C.M. Christianen, J.C. Maan, T. Wojtowicz, G. Karczewski, J. Kossut, *Phys. Status Solidi A* **178**, 33 (2000).
- [6] C.P. Poole, H.A. Farach, R.J. Creswick, *Superconductivity*, Academic Press, San Diego 2003.
- [7] W. Maslana, W. Mac, J.A. Gaj, P. Kossacki, A. Golnik, J. Cibert, S. Tatarenko, T. Wojtowicz, G. Karczewski, J. Kossut, *Phys. Rev. B, Condens. Matter* **63**, 165318 (2001).
- [8] P. Kossacki, H. Boukari, M. Bertolini, D. Ferrand, J. Cibert, S. Tatarenko, J.A. Gaj, B. Deveaud, V. Ciulin, M. Potemski, *Phys. Rev. B, Condens. Matter* **70**, 195337 (2004).
- [9] H.W. Weber, E. Seidl, C. Laa, E. Schachinger, M. Prohammer, A. Junod, D. Eckert, *Phys. Rev. B, Condens. Matter* **44**, 7585 (1991).
- [10] Z. Huai, J.W. Lynn, C.F. Majkrzak, S.K. Satija, J.H. Kang, X.D. Wu, *Phys. Rev. B, Condens. Matter* **52**, 10395 (1995).

- [11] K.S. Ilin, S.A. Vitusevich, B.B. Jin, A.I. Gubin, N. Klein, M. Siegel, *Physica C* **408-410**, 700 (2004).
- [12] J.R. Clem, *J. Low Temp. Phys.* **18**, 427 (1975).
- [13] A.A. Abrikosov, *Sov. Phys. JETP* **5**, 1174 (1957).
- [14] J.A. Gaj, W. Grieshaber, C. Bodin-Deshayes, J. Cibert, G. Feuillet, d.Y. Merle, A. Wasiela, *Phys. Rev. B, Condens. Matter* **50**, 5512 (1994).
- [15] C. Buss, R. Frey, C. Flytzanis, J. Cibert, *Solid State Commun.* **94**, 543 (1995).
- [16] S.J. Bending, *Adv. Phys.* **48**, 449 (1999).
- [17] B. König, I.A. Merkulov, D.R. Yakovlev, W. Ossau, S.M. Ryabchenko, M. Kutrowski, T. Wojtowicz, G. Karczewski, J. Kossut, *Phys. Rev. B, Condens. Matter* **61**, 16870 (2000).